Supplement of Atmos. Chem. Phys., 16, 10793–10808, 2016
http://www.atmos-chem-phys.net/16/10793/2016/
doi:10.5194/acp-16-10793-2016-supplement

Atmospheric Chemistry and Physics
Open Access
EGU

Supplement of

Impact of molecular structure on secondary organic aerosol formation from aromatic hydrocarbon photooxidation under low-NO_x conditions

Lijie Li et al.

Correspondence to: David R. Cocker III (dcocker@engr.ucr.edu)

Radical conditions are important to SOA formation (Ng, et al., 2007; Li, et al., 2015) and $RO_2\cdot$ and $HO_2\cdot$ reaction is a major pathway to SOA formation (Kroll and Seinfeld, 2008;). The NO conditions used in this work assure that $RO_2\cdot$ and $HO_2\cdot$ reaction is a major pathway during the oxidation of the aromatic studies (Fig. S1). The relationship of SOA yield to a number of radical parameters were analyzed based the average radical parameters during photooxidation (Table S4). $[HO_2\cdot]$ shows a correlation (0.35~0.4) with yield when C_8 and C_9 aromatic hydrocarbons are analyzed either all together or individually. Fig S2 shows the relationship of $[HO_2\cdot]$ to yield. Fig S2 is colored by substitute number or position and sized with mass loading M_0. Particle size generally grows larger from left to right demonstrating a positive correlation with M_0 and $[HO_2\cdot]$ (0.43, p-value=0.00). A similar size circle in each vertical slice illustrates SOA yield differences between isomers at similar $[HO_2\cdot]$ condition. Two typical slices are boxed to compare isomer SOA yield. The left slice shows that one substitute isomers (turquoise) form more SOA than three substitute ones (mustard) at similar mass loading and radical concentrations. The right slice shows that ortho position isomers (purple) yields are higher than para ones (red). Additionally, a trend showing that ortho position isomers (purple) have higher yield than the meta isomers when M_0>40 $\mu g\cdot m^{-3}$(larger size cycle) and 15-35*10^6 molecules$\cdot cm^{-3}$ $[HO_2\cdot]$. Radical analysis in general further supports the relationship found between SOA yield and precursor molecular structure.

It is further noticed that the low $[HO_2\cdot]$ and yield correlation is due to the difference in isomer k_{OH} (Table S1). It is found that k_{OH} correlates well with yield especially when only C_9 isomers are considered (-0.451, p-value=0.002). The inverse correlation explains that SOA yield hinges on molecular structure instead of kinetic reaction rate (Li, et al., 2016). The insignificant correlation between k_{OH} and C_8 isomers is due to a greater impact of molecular structure on SOA formation than $k_{OH.}$

Table S1 Aromatic hydrocarbon physical properties and rate constant

Compound	Vapor Pressure[a] mmHg	Boiling Point[b] °C	k_{OH}[c] 10^{-11} cm^3 $molecule^{-1}$ s^{-1}
Ethylbenzene	9.2	136	0.70
Propylbenzene	3.1	159	0.58
Isopropylbenzene	4.5	152	0.63
m-Xylene	9.0	139	2.31
o-Xylene	6.0	144	1.36
p-Xylene	7.9	138	1.43
m-Ethyltoluene	3.0	158	1.86
o-Ethyltoluene	2.6	164	1.19
p-Ethyltoluene	2.9	162	1.18
1,2,4-Trimethylbenzene	2.1	170	3.25
1,2,3-Trimethylbenzene	1.4	175	3.27
1,3,5-Trimethylbenzene	2.3	165	5.67

Note: a) vapor pressures are referred to Chemispider at 25 °C; b) boiling points are referred to Chemispider; c) OH reaction rate constants used in SAPRC-11 model at 25 °C ; *Predicted data from on Chemispider.

Table S2 Experiment conditions of additional aromatic hydrocarbon experiments

Precursor	ID	HC/NO ppbC:ppb	NO ppb	HC ppb	ΔHC μg·m^{-3}	M_0 μg·m^{-3}	Yield
m-xylene[1,3]	104A	10.1	64.4	81.3	328	21.7	0.07
	104B	29.3	21.4	78.4	281	20.4	0.07
	129A	15.1	45.5	86	336	21.9	0.07
	149A	13.3	50.2	83.6	342	52.8	0.15
	164A	12.4	44.0	68.0	271	16.8	0.06
	164B	12.2	44.1	67.5	270	14.6	0.05
	217A	36.8	8.90	40.9	155	9.80	0.06
	217B	35.9	8.70	39	153	7.90	0.05
	219A	63.7	7.00	55.7	165	9.20	0.06
	219B	67.5	6.60	55.7	166	9.30	0.06
	288A	63.1	7.00	55.2	183	9.00	0.05
	290A	31.1	15.3	59.5	229	9.00	0.04
	293A	29.9	13.7	51.2	189	9.20	0.05
	368A	17.9	21.0	47.0	149	6.90	0.05
	485A	17.5	43.3	94.7	353	37.2	0.11
	485B	16.7	45.0	93.7	349	40.4	0.12
	488A	15.5	46.2	89.6	341	29.5	0.09
	492A	13.6	44.3	75.2	296	29.1	0.10
	492B	13.5	44.8	75.5	298	29.7	0.10
	566A	14.0	48.3	84.5	337	48.2	0.14
	566B	13.3	48.0	79.8	318	48.4	0.15
	758A	47.5	11.4	67.7	158	13.5	0.09
	820A	30.2	20.7	78.1	260	17.0	0.07
	1193A	15.5	36.8	71.1	239	13.6	0.06
	1193B	15.2	36.5	69.5	236	11.2	0.05
	1191A	12.6	52.2	82.1	298	15.2	0.05
	1191B	14.6	45.7	83.6	340	14.6	0.04
	1516A	27.8	26.7	92.9	357	48.7	0.14
	1950A	14.1	45.5	80.0	327	26.3	0.08
	1950B	14.6	45.9	83.6	345	28.7	0.08
o-xylene[2]	503B	15.5	75.0	145	448	30.0	0.07
	505A	171	48.0	1026	360	32.0	0.09
	508A	17.9	24.3	54.3	208	12.5	0.06
	517B	30.9	26.8	103.7	296	32.0	0.11
	522A	8.80	52.0	57.1	220	7.70	0.04
	522B	41.7	11.0	57.4	171	15.0	0.09
p-xylene[2]	422B	33.1	23.9	98.8	211	5.90	0.03
	502A	41.0	21.0	108	292	19.0	0.07
	503A	18.0	75.0	169	579	66.0	0.11
	504A	16.3	129	263	876	103	0.12
	504B	15.8	131	260	675	52.0	0.08
	515B	18.5	26.0	60.3	200	8.00	0.04
	519B	29.2	53.0	194	450	36.5	0.08

	525A	45.3	10.2	57.8	163	8.0	0.05
1, 2, 4-trimethylbenzene	1117A	69.8	10.3	80.0	335	16.8	0.05
	1117B	34.8	20.7	80.0	368	18.2	0.05
	1119A	14.1	49.8	78.0	385	19.6	0.05
	1119B	17.1	41.6	79.0	390	25.5	0.07
	1123A	71.0	10.1	80.0	300	11.2	0.04
	1123B	32.6	22.1	80.0	345	15.4	0.05
	1126A	69.3	10.1	77.5	286	12.6	0.04
	1126B	28.1	24.3	75.9	333	15.4	0.05
	1129B	24.2	15.6	42.0	201	5.60	0.03

Table S3. Two product yield curve fitting parameters for selected compounds

Yield Curve	α_1	$K_{om,1}$ ($m^3 \cdot \mu g^{-1}$)	α_2	$K_{om,2}$ ($m^3 \cdot \mu g^{-1}$)
Ethylbenzene	0.160	0.039	0.138	0.005
Propylbenzene (i- and n-)	0.117	0.040	0.139	0.005
o-Xylene	0.141	0.025	0.264	0.005
o-Ethyltoluene	0.173	0.024	0.247	0.005
m-Xylene	0.166	0.036	0.083	0.005
m-Ethyltoluene	0.152	0.036	0.085	0.005
p-Xylene	0.168	0.026	0.016	0.005
p-Ethyltoluene	0.144	0.022	0.049	0.005

Table S4 Average radical concentrations during photooxidation

Run ID	RO_2[a]	HO_2[a]	OH[b]	HO_2*RO[c]	HO_2/RO_2	NO/HO_2	OH/HO_2[d]	NO_3[a]
1142A	17.0	13.78	9.21	474	1.50	4.0E+04	1.5E-01	9.60
1142B	1.38	3.08	5.61	12.6	2.16	3.6E+05	4.8E-01	15.9
1146A	11.3	14.07	4.52	225	1.60	6.9E+02	2.0E-02	4.21
1146B	14.8	14.68	6.91	340	1.42	6.0E+03	5.0E-02	5.92
2084A	12.5	16.99	1.91	257	1.60	1.2E+02	3.7E-03	1.62
2084B	10.1	15.07	1.62	189	1.72	1.4E+02	3.7E-03	1.36
1245A	8.22	10.66	4.17	132	1.49	2.3E+03	3.0E-02	4.75
1246A	8.71	9.03	4.28	194	1.55	2.1E+05	2.3E-01	24.8
1247A	15.6	15.48	5.21	338	1.38	7.6E+02	2.0E-02	3.04
1247B	11.2	10.99	7.56	280	1.62	2.5E+07	2.3E+01	9.12
1253A	23.7	20.12	6.47	726	1.23	2.1E+05	4.3E-01	5.18
1253B	4.24	6.74	5.02	100	2.00	1.1E+05	1.6E-01	28.4
1193A	11.0	12.33	3.14	185	1.34	1.5E+06	1.8E+00	14.0
1193B	8.97	11.59	2.82	141	1.44	3.2E+05	4.2E-01	18.7
1191A	19.1	15.83	5.81	449	1.23	4.5E+05	3.4E-01	32.1
1191B	10.8	12.43	2.36	189	1.46	3.8E+04	5.1E-02	18.5
1516A	18.6	23.1	3.14	465	1.33	1.5E+01	2.0E-03	2.37
1950A	11.7	20.62	4.46	267	1.84	7.2E+01	4.3E-03	38.4
1950B	13.3	22.03	4.64	326	1.74	4.6E+01	3.7E-03	37.1
1315A	17.5	20.7	8.28	495	1.52	1.0E+03	1.8E-02	28.9
1315B	19.8	21.59	5.20	478	1.23	3.5E+01	4.3E-03	3.38
1320A	53.2	21.02	11.9	1432	0.79	3.7E+02	1.7E-02	1.77
1321A	21.0	21.35	5.14	506	1.20	3.1E+01	4.1E-03	2.46
1321B	22.9	19.43	3.58	484	1.02	4.3E+00	2.1E-03	0.72
1308A	12.5	13.89	7.04	308	1.40	2.0E+05	3.9E-01	15.9
1308B	24.0	18.01	5.66	564	1.00	1.0E+03	1.6E-02	3.36
1151A	8.97	14.15	9.27	251	0.00	2.4E+04	8.0E-02	66.7
1151B	23.3	22.14	9.83	788	1.40	5.6E+03	3.6E-02	13.3
1199A	15.1	22.49	4.16	373	1.57	8.1E+01	4.0E-03	24.0
1222B	20.3	27.24	8.11	625	1.15	9.7E+01	4.1E-03	55.5
1226B	24.3	32.15	5.66	885	1.44	3.2E+02	5.8E-03	105
1232A	22.2	30.55	4.57	774	1.52	2.3E+02	4.4E-03	104
1421A	20.0	22.36	3.05	504	1.30	3.7E+00	1.5E-03	2.43
1421B	23.2	27.06	6.33	710	1.30	2.3E+01	3.6E-03	13.7
1179A	12.6	17.6	5.26	294	1.72	3.9E+02	1.0E-02	51.5
1179B	14.0	19.05	5.50	329	1.60	2.2E+02	8.2E-03	51.1
1202A	13.8	17.77	5.94	350	1.57	8.5E+03	3.9E-02	39.6
1215A	25.7	25.73	6.06	981	1.47	3.3E+03	1.8E-02	53.1
1413A	19.1	20.64	3.54	430	1.17	1.7E+01	2.6E-03	3.00
1413B	20.9	22.76	6.96	550	1.24	2.1E+02	8.7E-03	19.4
1194A	23.1	20.6	3.85	675	1.16	5.1E+04	5.9E-02	37.4
1194B	23.5	20.04	4.10	712	1.19	3.9E+04	5.3E-02	26.4
1197A	25.2	20.97	3.60	733	1.13	1.8E+04	4.0E-02	5.61
1197B	24.6	19.92	5.18	782	1.04	1.0E+08	3.7E+01	20.5
1214B	22.3	18.34	7.57	623	1.16	6.4E+03	4.3E-02	14.4
1601A	36.8	31.89	9.25	1489	0.99	9.7E+06	2.1E+01	6.21
1158A	20.1	18.64	1.68	391	1.04	4.2E+00	1.0E-03	1.35
1158B	43.4	21.98	3.49	957	0.72	2.9E-01	1.6E-03	1.28

1162A	19.7	23.94	4.75	523	1.42	7.9E+00	2.4E-03	37.2
1162B	96.9	19.22	5.78	1445	0.44	3.8E-02	3.5E-03	0.33
1117A	13.1	15.79	1.69	220	1.29	1.2E+01	1.5E-03	7.29
1117B	9.83	14.58	2.49	172	1.58	1.9E+02	4.7E-03	34.9
1119A	12.5	18.77	5.29	300	1.66	2.7E+03	1.7E-02	89.0
1119B	12.1	17.26	3.95	296	1.86	2.9E+03	1.7E-02	68.7
1123A	15.9	15.09	1.66	274	1.06	6.8E+01	2.2E-03	2.91
1123B	15.8	18.56	2.54	321	1.22	7.7E+01	3.0E-03	23.2
1126A	17.3	17.63	1.69	324	1.07	1.7E+01	1.5E-03	4.26
1126B	29.9	24.76	7.50	841	1.03	3.2E+01	3.8E-03	33.7
1129B	11.2	15.45	4.29	199	1.58	5.6E+01	4.9E-03	24.0
1153A	14.9	18.64	1.10	292	1.28	1.2E+01	8.3E-04	1.22
1153B	17.5	21.78	1.99	411	0.00	1.6E+01	1.3E-03	3.33
1156A	11.1	19.85	2.08	249	1.97	2.5E+01	1.6E-03	31.8
1156B	9.86	19.63	2.85	218	2.18	6.1E+01	2.8E-03	54.4
1329B	2.51	9.07	4.45	26.0	4.62	2.2E+02	8.0E-03	125

Note: average radical concentrations are calculated by dividing time integrated radical parameters with photooxidation time; average radical concentration throughout photooxidation a) in 10^6 molecules·cm^{-3}; b) in 10^8 molecules·cm^{-3}; c) in 10^{16}molecules·cm^{-3}; d) average radical ratio throughout photooxidation in 10^3

Table S5 Correlation between SOA yields and average radical concentrations

C_8 &C_9	RO_2	HO_2	OH	HO_2*RO_2	HO_2/ RO_2	NO/HO_2	OH/HO_2	NO_3
Yield	0.152	0.393	-0.046	0.24	-0.099	-0.046	-0.108	0.093
p-value[a]	0.223	0.001	0.714	0.053	0.428	0.712	0.388	0.457

C_9	RO_2	HO_2	OH	HO_2*RO_2	HO_2/ RO_2	NO/HO_2	OH/HO_2	NO_3
Yield	0.189	0.376	0.098	0.303	-0.133	-0.07	-0.141	0.094
p-value[a]	0.208	0.010	0.516	0.040	0.380	0.644	0.349	0.535

C_8	RO_2	HO_2	OH	HO_2*RO_2	HO_2/ RO_2	NO/HO_2	OH/HO_2	NO_3
Yield	-0.092	0.353	-0.386	-0.094	0.200	-0.293	-0.318	-0.278
p-value[a]	0.699	0.127	0.093	0.693	0.398	0.209	0.171	0.235

Note: C_8 &C_9 correlation analysis used all the experiments listed in Table S4, C_8 or C_9 correlation analysis only used C_8 or C_9 isomer experiments listed in Table S4. a) P-values range from 0 to 1, 0-reject null hypothesis and 1 accept null hypothesis. Alpha (α) level used is 0.05. If the p-value of a test statistic is less than alpha, the null hypothesis is rejected

Table S6. SOA Fragments in HR-TOF-AMS at m/z 43, 57 and 71*

Compound	**m/z**					
	43		44	57		71
	$C_2H_3O^+$	$C_3H_7^+$	CO_2^+	$C_3H_5O^+$	$C_4H_9^+$	$C_4H_7O^+$
Ethylbenzene	×		×	×		
Propylbenzene	×	×	×	×	×	×
Isopropylbenzene	×	×	×	×		×
m-Xylene	×		×			
m-Ethyltoluene	×		×	×		
o-Xylene	×		×			
o-Ethyltoluene	×		×	×		
p-Xylene	×		×			
p-Ethyltoluene	×		×	×		
1,2,3-Trimethylbenzene	×		×	×		
1,2,4-Trimethylbenzene	×			×		
1,3,5-Trimethylbenzene	×		×	×		

* Experimental runs same as Fig. S4.

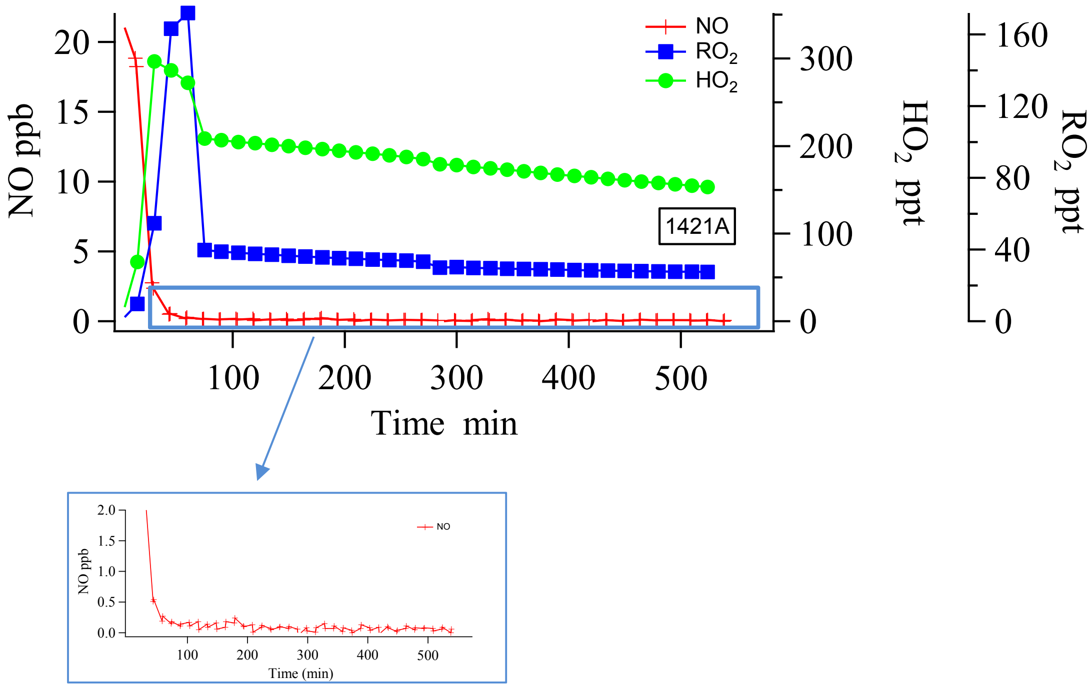

(a)

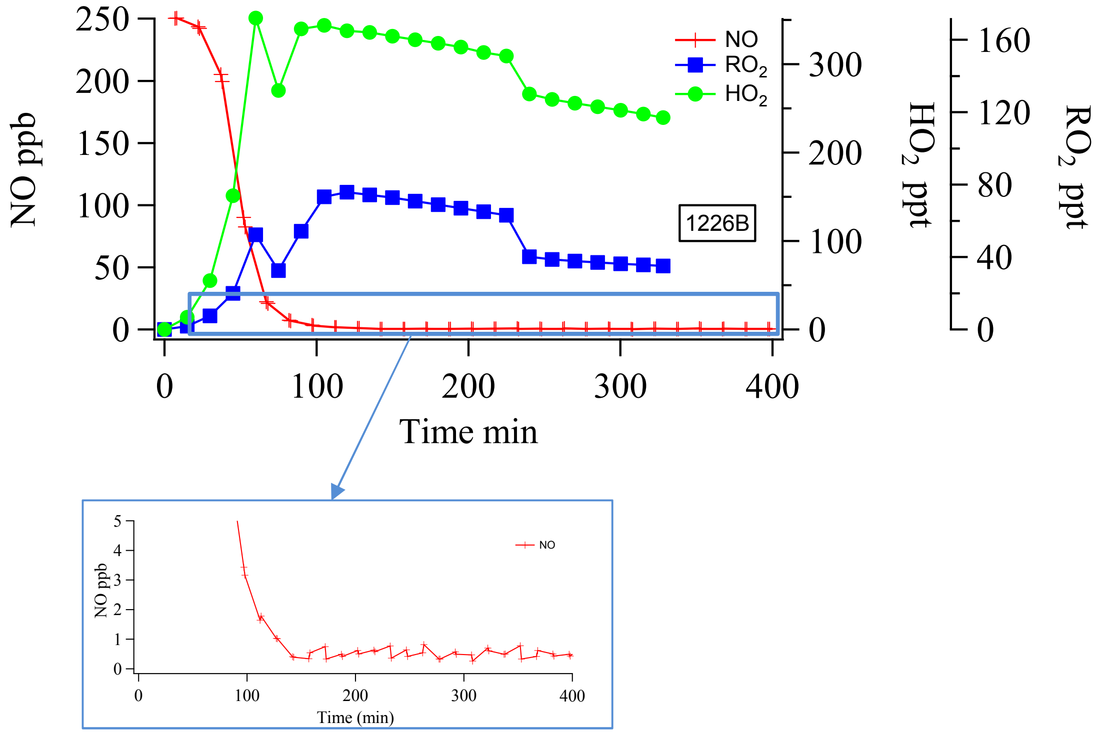

(b)

Fig. S1 Time series concentration change of NO, $HO_2\cdot$ and $RO_2\cdot$ during the phototoxidation of aromatic hydrocarbons. (m-Ethyltoluene, 1226B and 1421A; radical concentrations are predicted by SAPRC-11, Lower Left Panel: Zoom in NO concentration)

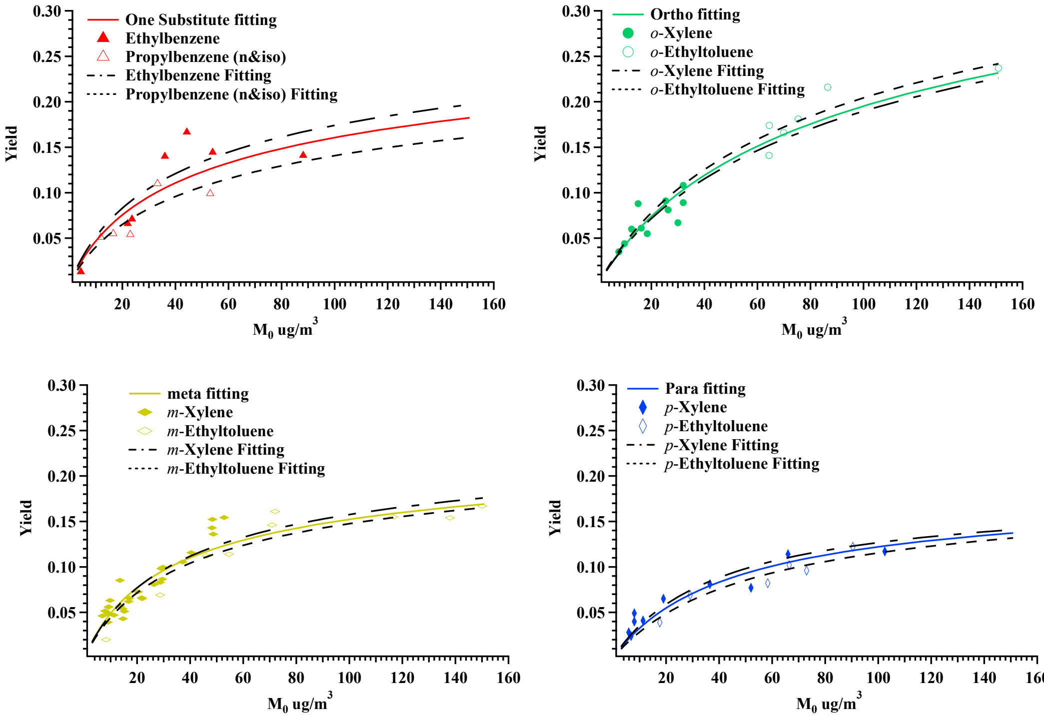

Fig. S2 Aromatic SOA yields as a function of M_0 for single compounds: a) Ethylbenzene (dotted line) vs Propylbenzene (i- and n-)(dashed line); b) *o*-Xylene(dotted line) vs *o*-Ethyltoluene(dashed line); c) *m*-Xylene(dotted line) vs *m*-Ethyltoluene(dashed line); d) *p*-Xylene (dotted line) vs *p*-Ethyltoluene (dashed line) (Note: Song, et al, 2005; Song, et al, 2007; Li, et al., 2016 data are also included)

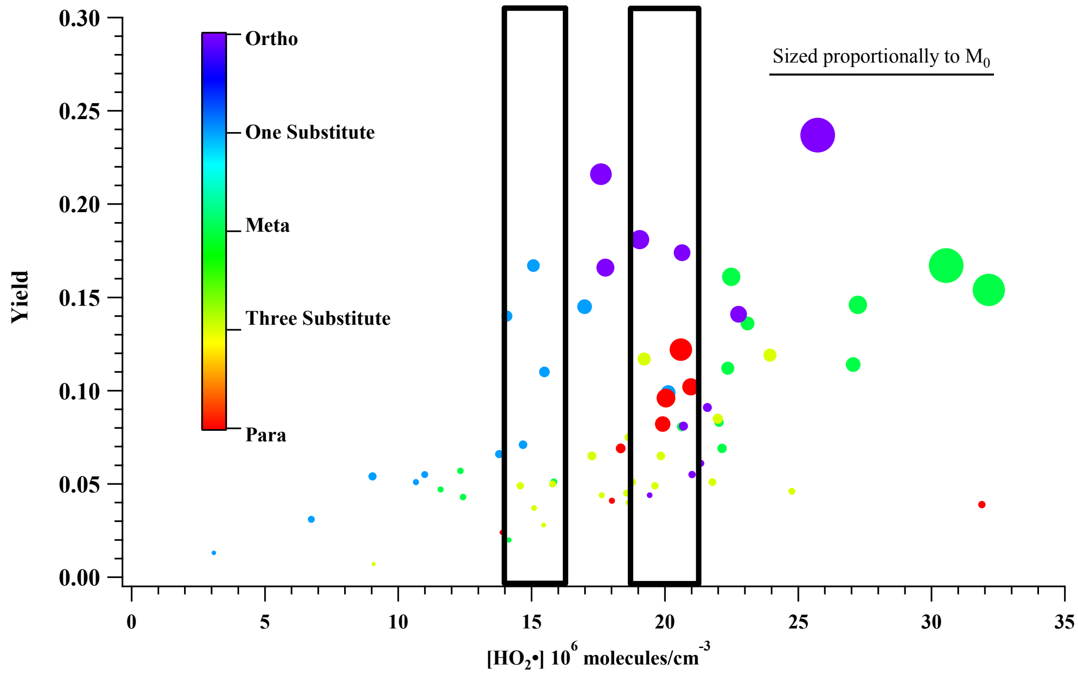

Fig. S3 Relationship between SOA yield and $HO_2\cdot$ radical concentration (Colored with substitute number or position and sized with mass loading M_0)

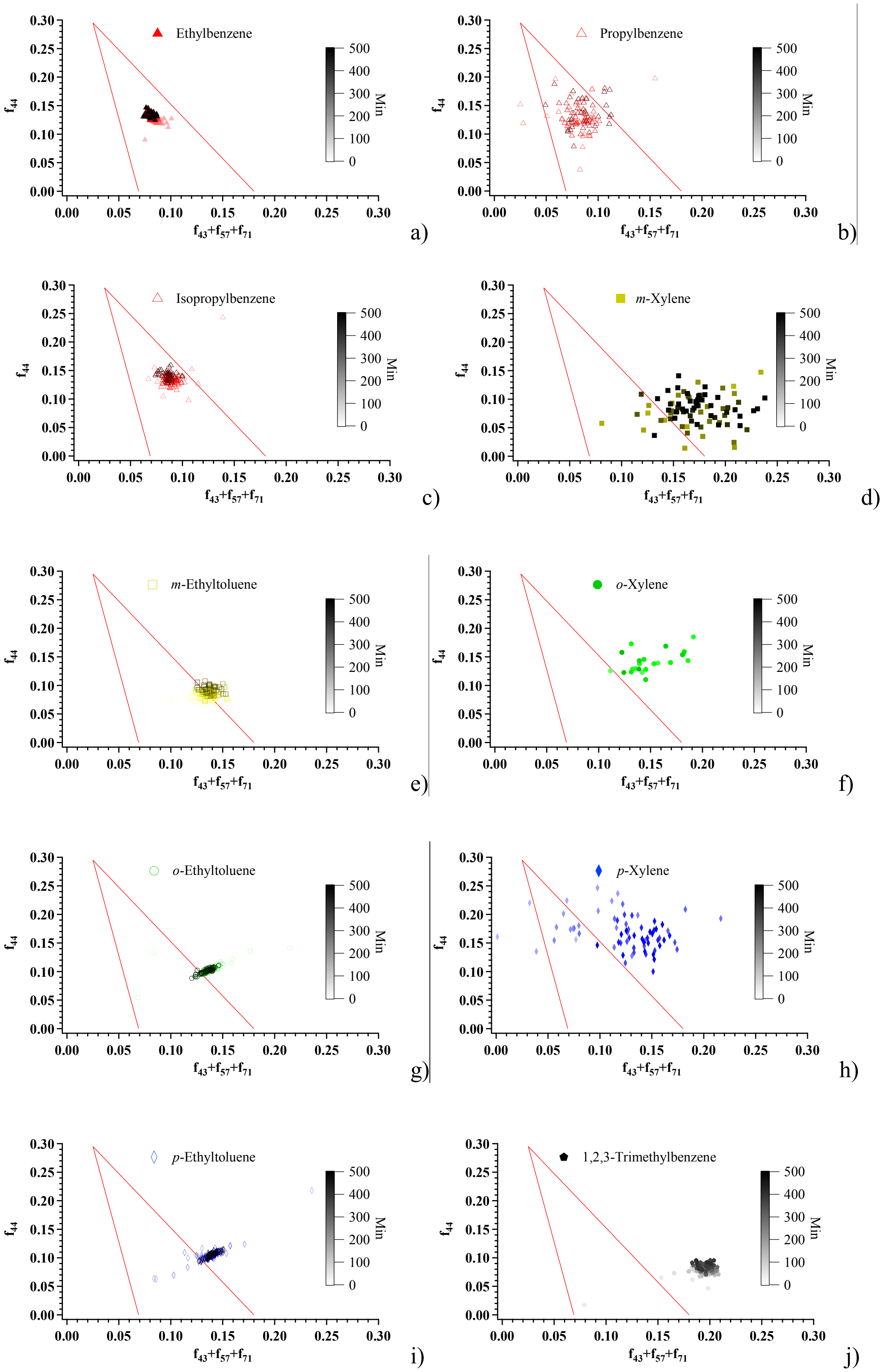
Ethylbenzene
a)
Propylbenzene
b)
Isopropylbenzene
c)
m-Xylene
d)
m-Ethyltoluene
e)
o-Xylene
f)
o-Ethyltoluene
g)
p-Xylene
h)
p-Ethyltoluene
i)
1,2,3-Trimethylbenzene
j)
f44
f43+f57+f71
0.00 0.05 0.10 0.15 0.20 0.25 0.30
Min
500 400 300 200 100 0

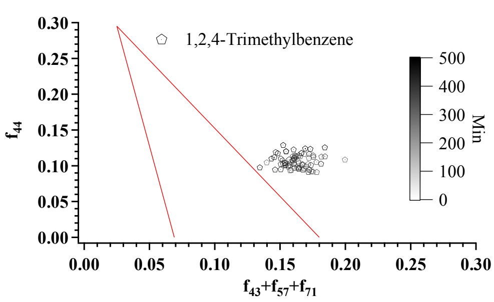

k)

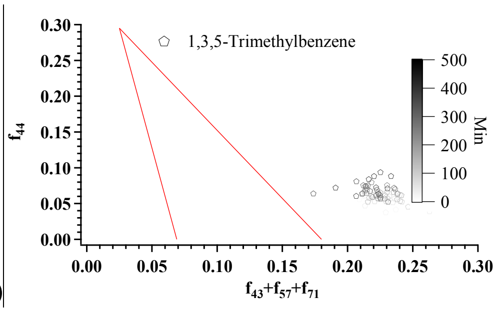

l)

Fig. S4 $f_{44+}$and $f_{43+57+71}$ evolution in SOA formed from different aromatic hydrocarbon photooxidation under low NO_x ; each marker type represents one aromatic hydrocarbon and marker is colored with photooxidation time from light to dark: a) Ethylbenzene 2048A; b) Propylbenzene 1245A; c) Isopropylbenzene 1247A; d) *m*-Xylene 1191A; e) *m*-Ethyltoluene 1199A; f) *o*-Xylene 1320A; g) *o*-Ethyltoluene 1179A; h) *p*-Xylene 1308A; i) *p*-Ethyltoluene 1194A; j) 1,2,3-Trimethylbenzene 1162A; k) 1,2,4-Trimethylbenzene 1119A; l) 1,3,5-Trimethylbenzene 1156A

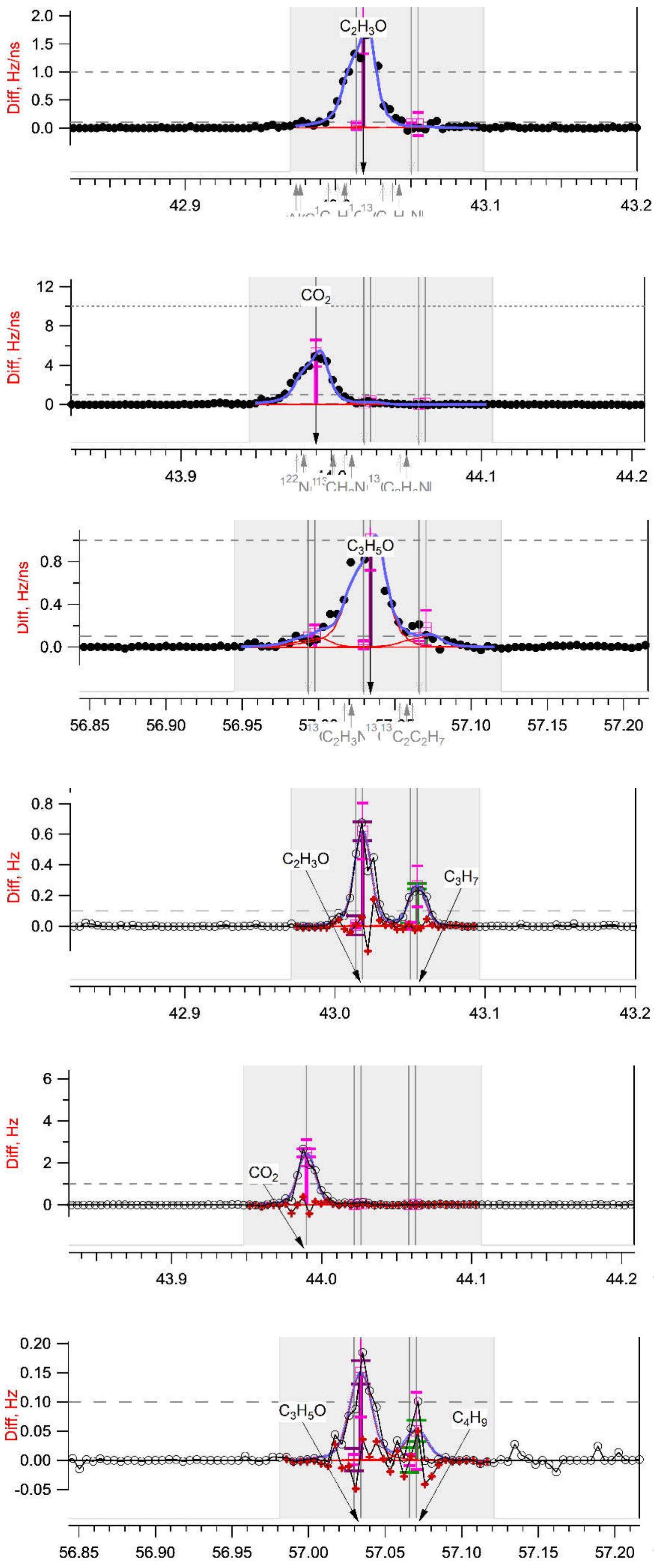

a-1)

a-2)

a-3)

b-1)

b-2)

b-3)

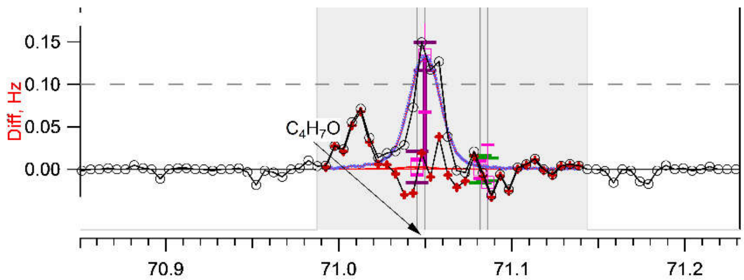
Diff, Hz
0.15
0.10
0.05
0.00
C4H7O
70.9
71.0
71.1
71.2

b-4)

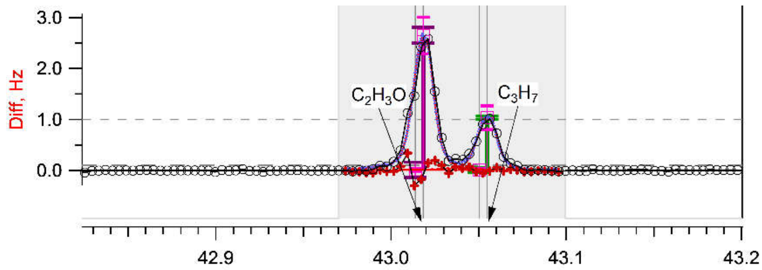
Diff, Hz
3.0
2.0
1.0
0.0
C2H3O
C3H7
42.9
43.0
43.1
43.2

c-1)

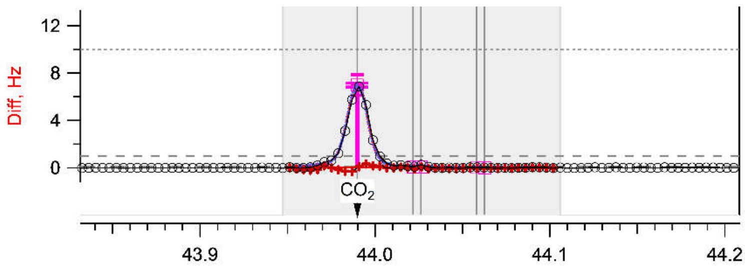
Diff, Hz
12
8
4
0
CO2
43.9
44.0
44.1
44.2

c-2)

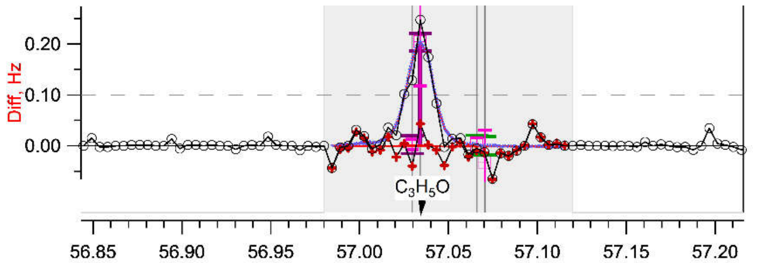
Diff, Hz
0.20
0.10
0.00
C3H5O
56.85
56.90
56.95
57.00
57.05
57.10
57.15
57.20

c-3)

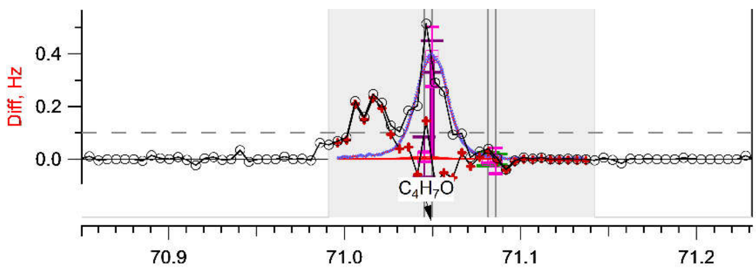
Diff, Hz
0.4
0.2
0.0
C4H7O
70.9
71.0
71.1
71.2

c-4)

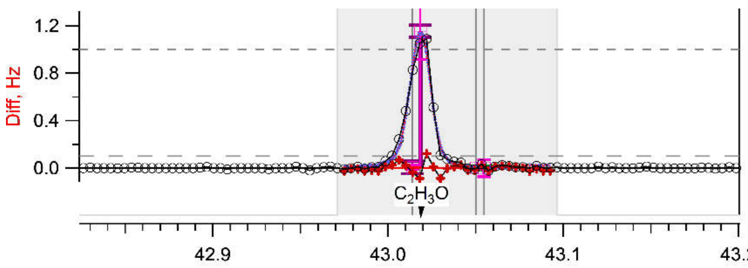
Diff, Hz
1.2
0.8
0.4
0.0
C_2H_3O
42.9
43.0
43.1
43.2

d-1)

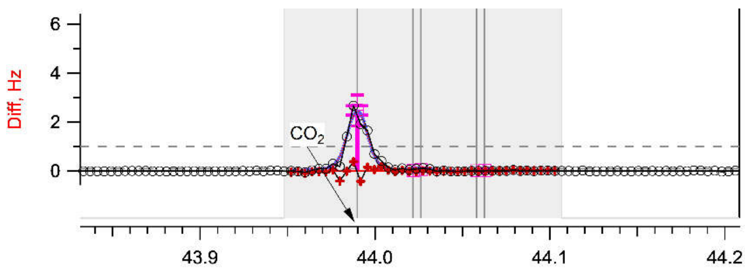
Diff, Hz
6
4
2
0
CO_2
43.9
44.0
44.1
44.2

d-2)

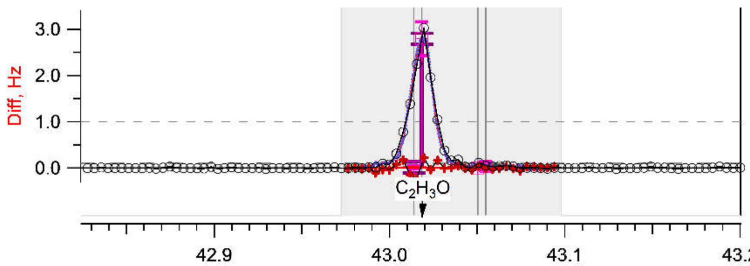
Diff, Hz
3.0
2.0
1.0
0.0
C_2H_3O
42.9
43.0
43.1
43.2

e-1)

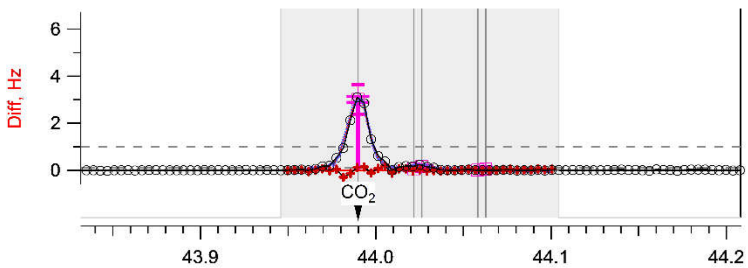
Diff, Hz
6
4
2
0
CO_2
43.9
44.0
44.1
44.2

e-2)

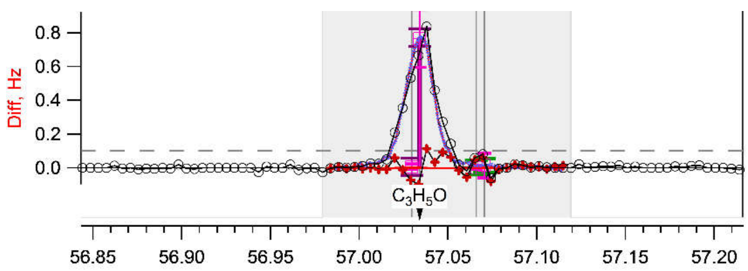
Diff, Hz
0.8
0.6
0.4
0.2
0.0
C_3H_5O
56.85
56.90
56.95
57.00
57.05
57.10
57.15
57.20

e-3)

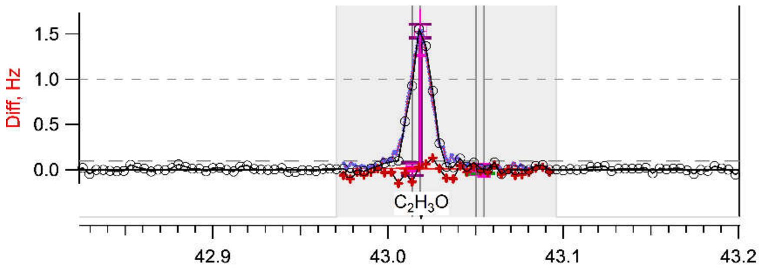

Diff, Hz
1.5
1.0
0.5
0.0
C2H3O
42.9
43.0
43.1
43.2

f-1)

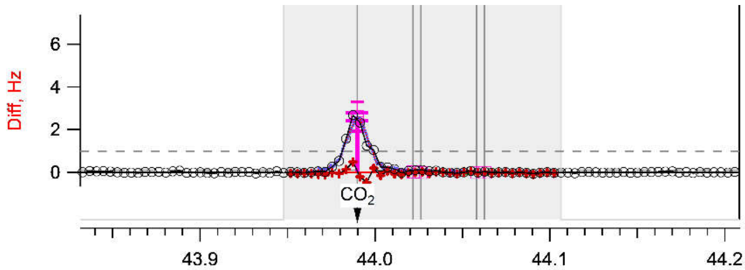

Diff, Hz
6
4
2
0
CO2
43.9
44.0
44.1
44.2

f-2)

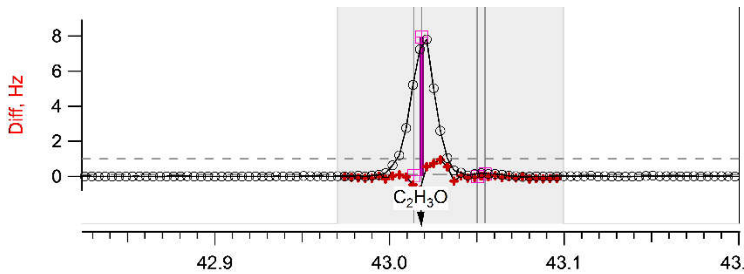

Diff, Hz
8
6
4
2
0
C2H3O
42.9
43.0
43.1
43.2

g-1)

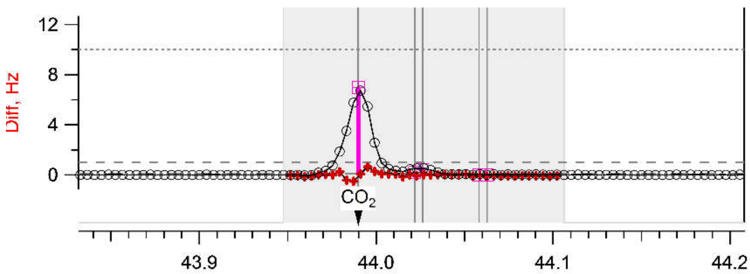

Diff, Hz
12
8
4
0
CO2
43.9
44.0
44.1
44.2

g-2)

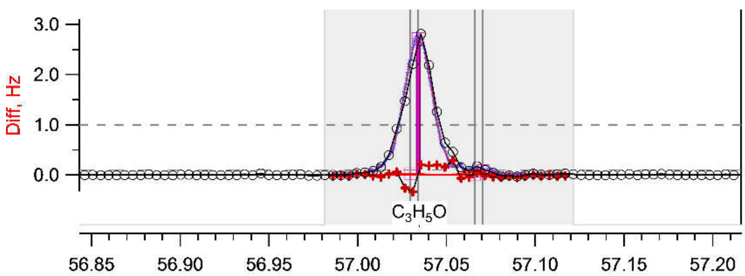

Diff, Hz
3.0
2.0
1.0
0.0
C3H5O
56.85
56.90
56.95
57.00
57.05
57.10
57.15
57.20

g-3)

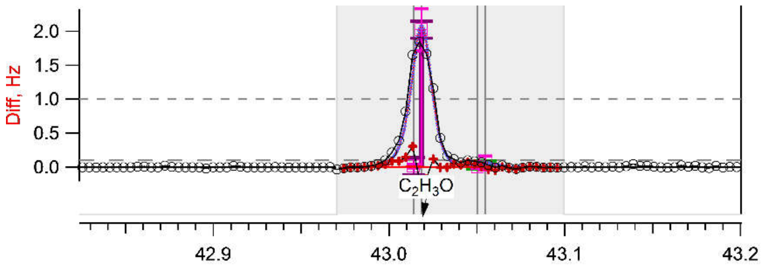
Diff, Hz
2.0
1.5
1.0
0.5
0.0
C_2H_3O
42.9
43.0
43.1
43.2

h-1)

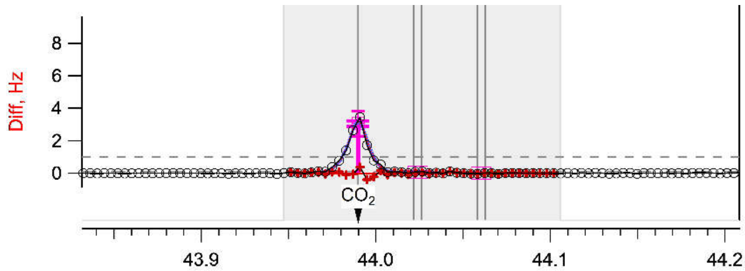
Diff, Hz
8
6
4
2
0
CO_2
43.9
44.0
44.1
44.2

h-2)

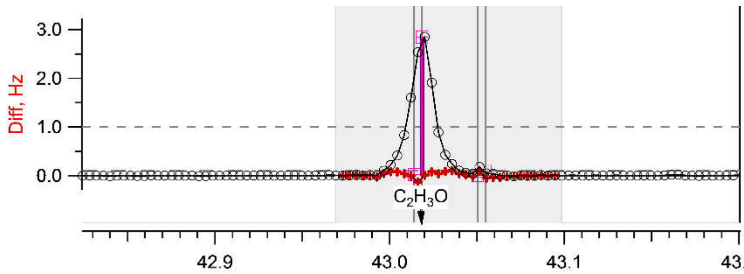
Diff, Hz
3.0
2.0
1.0
0.0
C_2H_3O
42.9
43.0
43.1
43.2

i-1)

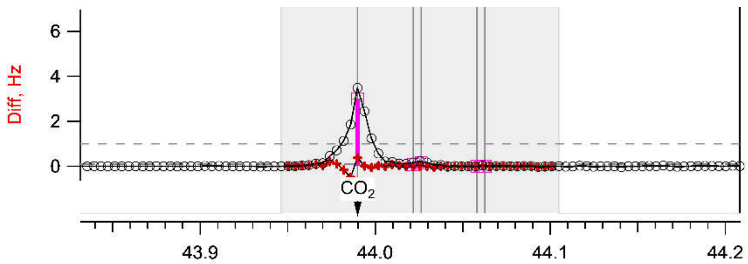
Diff, Hz
6
4
2
0
CO_2
43.9
44.0
44.1
44.2

i-2)

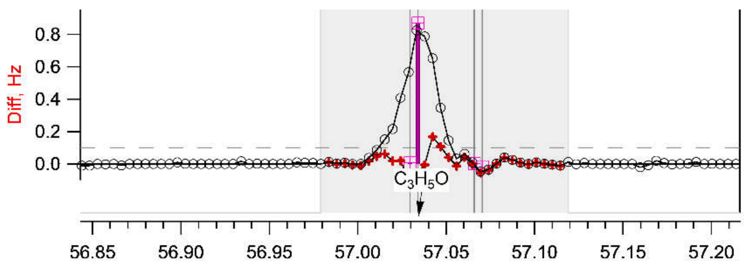
Diff, Hz
0.8
0.6
0.4
0.2
0.0
C_3H_5O
56.85
56.90
56.95
57.00
57.05
57.10
57.15
57.20

i-3)

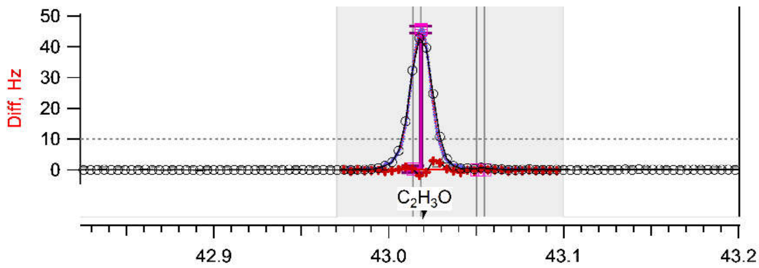
Diff, Hz
50
40
30
20
10
0
C2H3O
42.9
43.0
43.1
43.2
j-1)

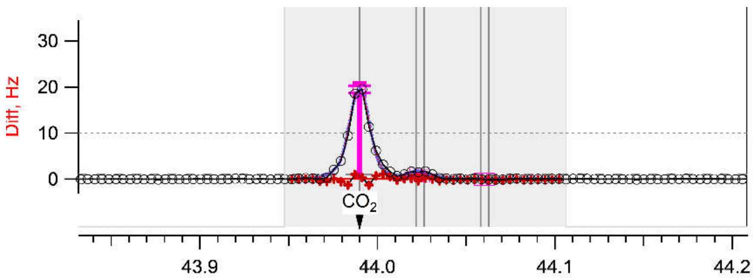
Diff, Hz
30
20
10
0
CO2
43.9
44.0
44.1
44.2
j-2)

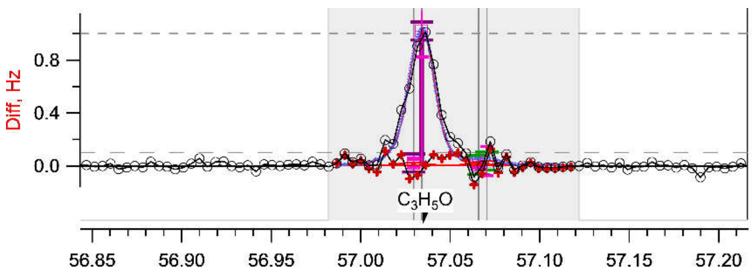
Diff, Hz
0.8
0.4
0.0
C3H5O
56.85
56.90
56.95
57.00
57.05
57.10
57.15
57.20
j-3)

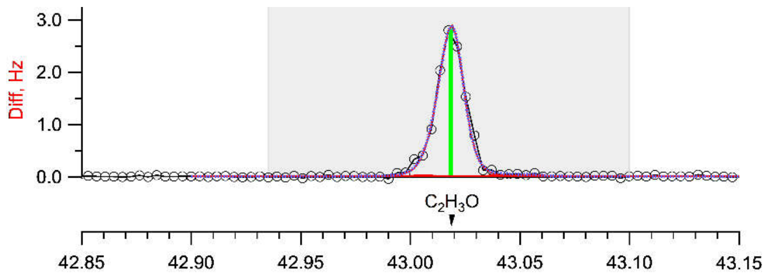
Diff, Hz
3.0
2.0
1.0
0.0
C2H3O
42.85
42.90
42.95
43.00
43.05
43.10
43.15
k-1)

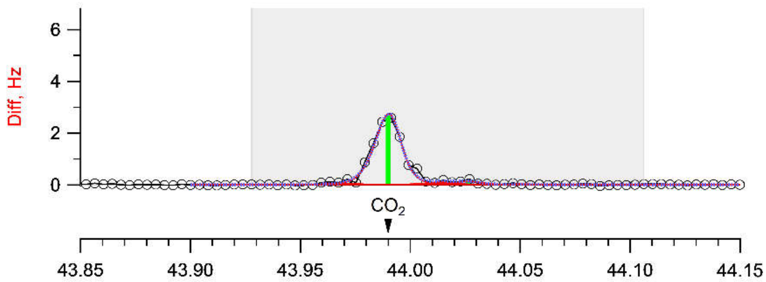
Diff, Hz
6
4
2
0
CO2
43.85
43.90
43.95
44.00
44.05
44.10
44.15
k-2)

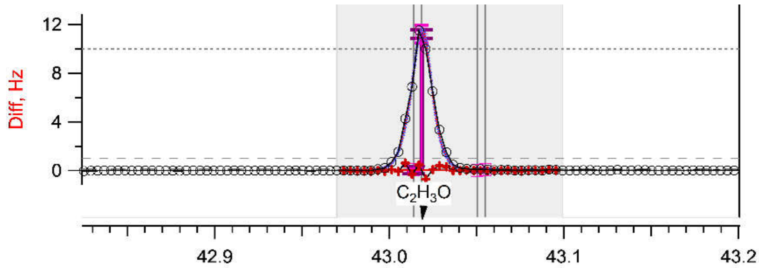

l-1)

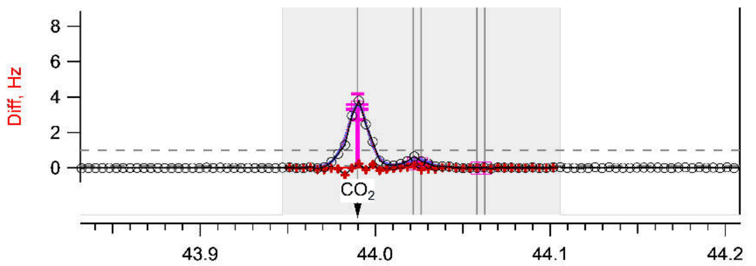

l-2)

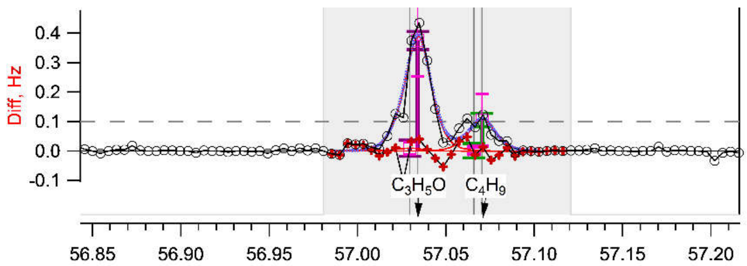

l-3)

Fig. S5 High-resolution mass spectra of m/z 43, m/z 44, m/z 57 and m/z 71 measured for secondary organic aerosol formed at peak aerosol concentration during aromatic photooxidation a) Ethylbenzene 1146A; b) Propylbenzene 1245A; c) Isopropylbenzene 1247A; d) *m*-Xylene 1191A; e) *m*-Ethyltoluene 1199A; f) *o*-Xylene 1320A; g) *o*-Ethyltoluene 1179A; h) *p*-Xylene 1308A; i) *p*-Ethyltoluene 1194A; j) 1,2,3-Trimethylbenzene 1162A; k) 1,2,4-Trimethylbenzene 1119A; l) 1,3,5-Trimethylbenzene 1156A (m/z 57 only includes $C_3H_5O^+$). *m/z peaks with intensity less than 0.1 are not displayed

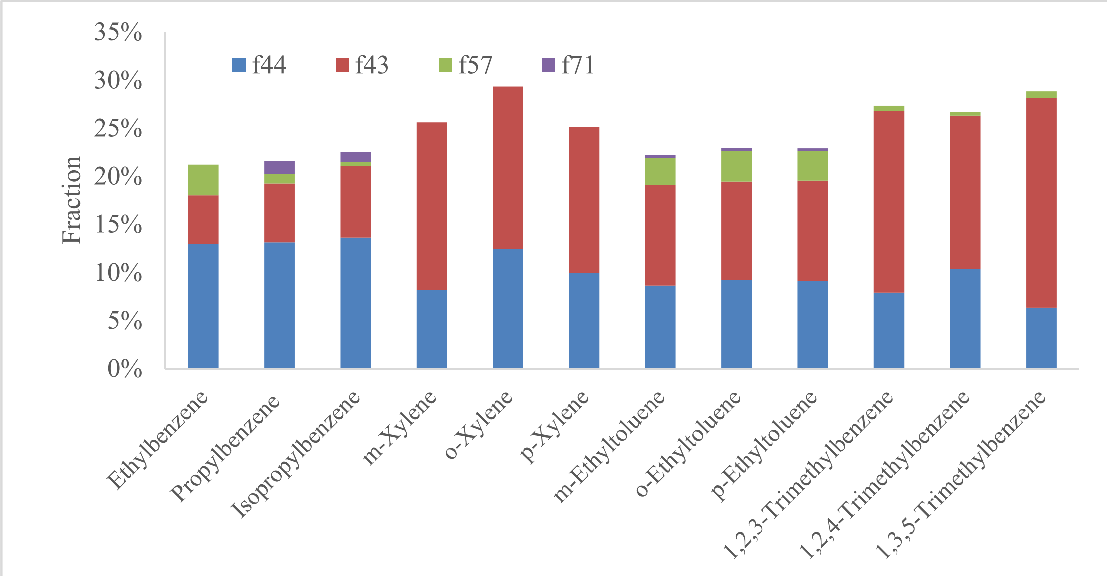

Fig. S6 m/z 43, m/z 44, m/z 57 and m/z 71 fraction in SOA formed from aromatic hydrocarbon photooxidation

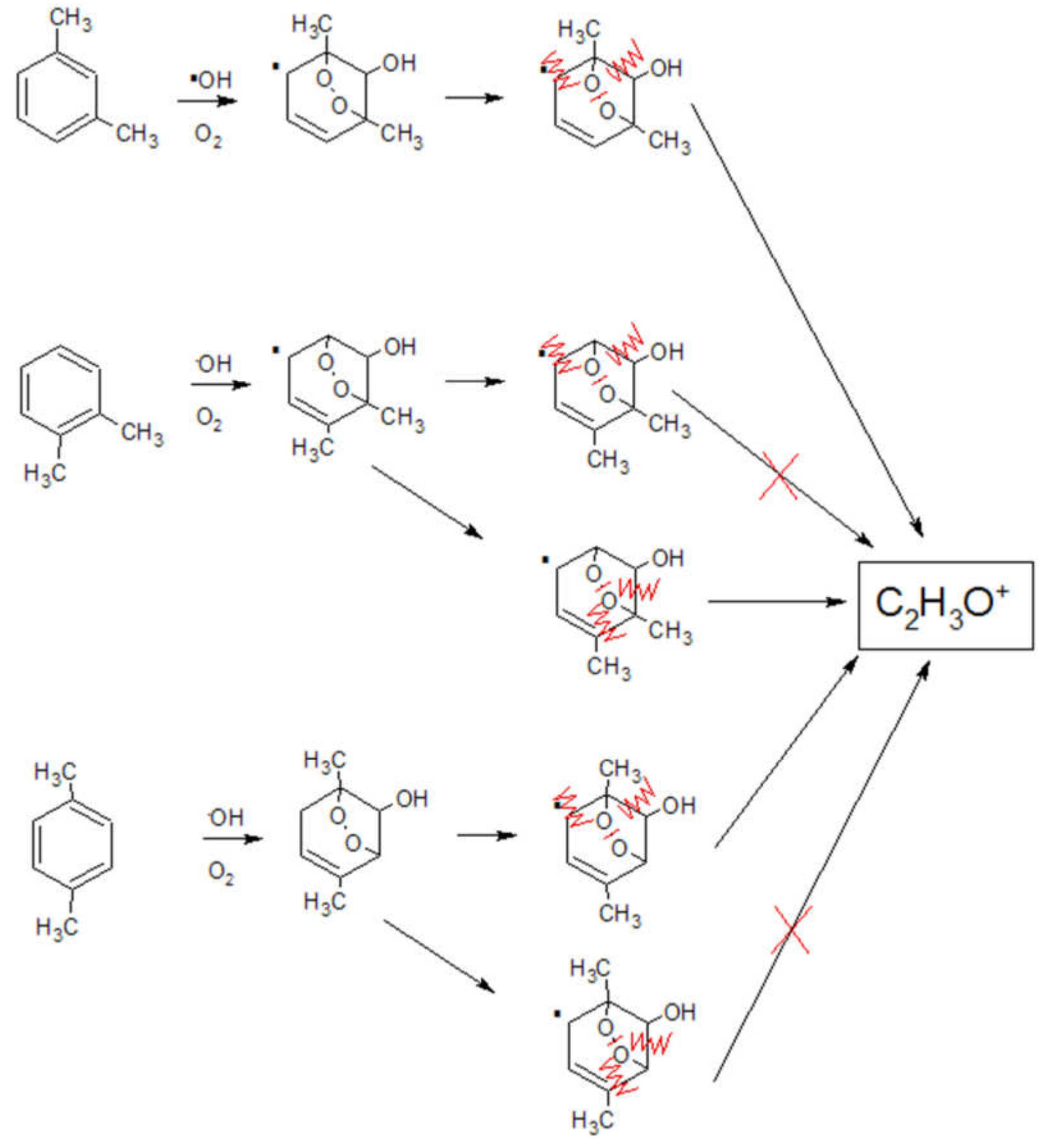

* Oxidation products of the bicyclic radicals lead to the formation of $C_2H_3O^+$. The bicyclic radicals show the origin of $C_2H_3O^+$ during the oxidation of aromatic hydrocarbons.

Fig. S7 The potential relationship between alkyl substitute location and the $C_2H_3O^+$ fragments from HR-TOF-AMS.

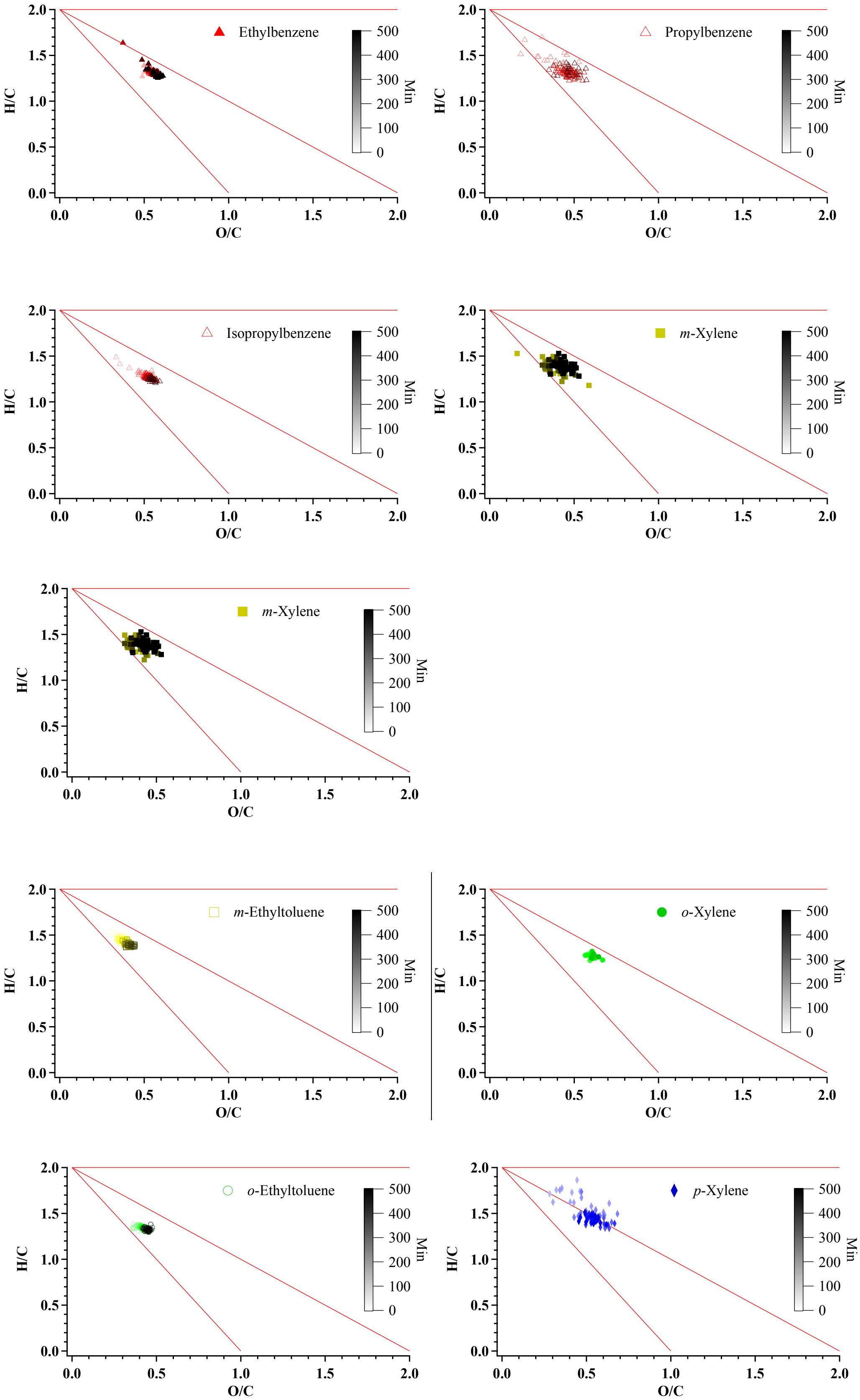

Ethylbenzene
Propylbenzene
Isopropylbenzene
m-Xylene
m-Xylene
m-Ethyltoluene
o-Xylene
o-Ethyltoluene
p-Xylene
H/C
O/C
Min
0.0
0.5
1.0
1.5
2.0
0
100
200
300
400
500

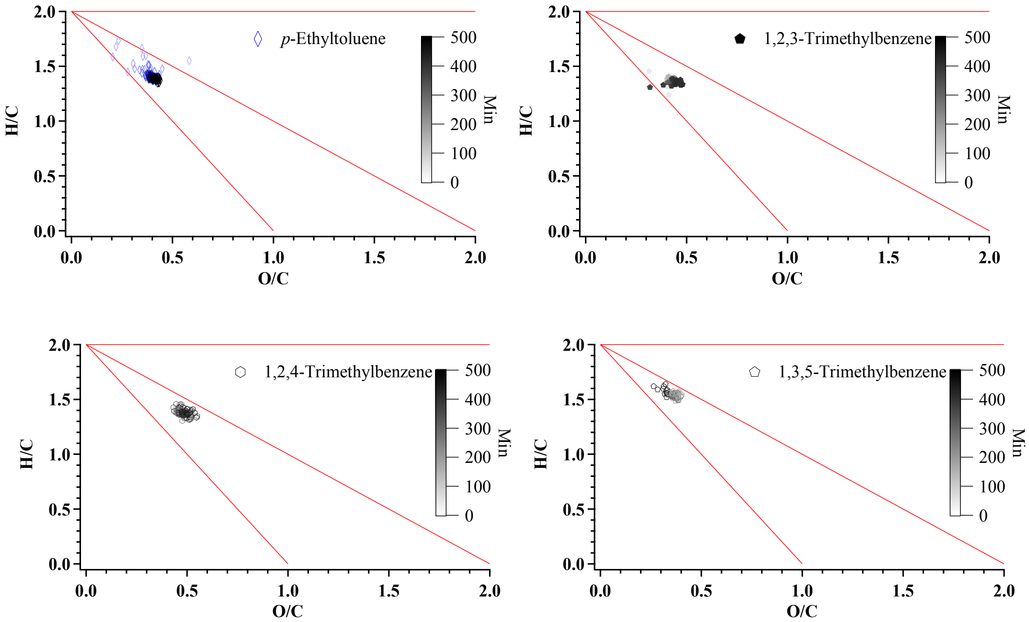

Fig. S8 H/C and O/C evolution in SOA formed from different aromatic hydrocarbon photooxidation under low NO_x; each marker type represents one aromatic hydrocarbon and marker is colored with photooxidation time from light to dark: a) Ethylbenzene 1146A; b) Propylbenzene 1245A; c) Isopropylbenzene 1247A; d) *m*-Xylene 1191A; e) *m*-Ethyltoluene 1199A; f) *o*-Xylene 1320A; g) *o*-Ethyltoluene 1179A; h) *p*-Xylene 1308A; i) *p*-Ethyltoluene 1194A; j) 1, 2, 3-Trimethylbenzene 1162A; k) 1, 2, 4-Trimethylbenzene 1119A; l) 1, 3, 5-Trimethylbenzene 1156A.

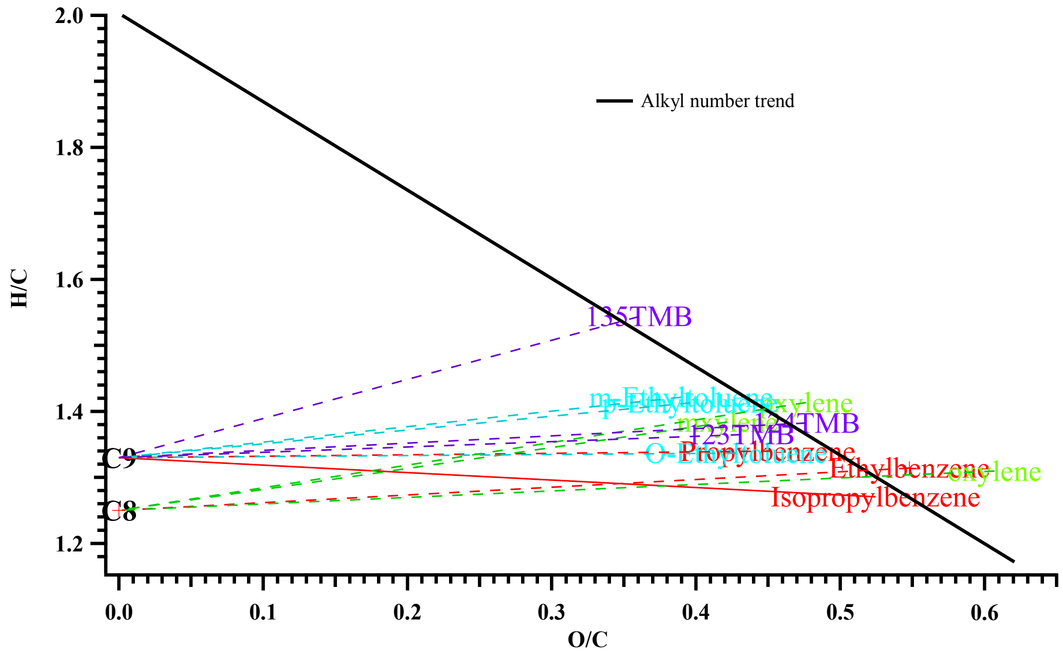

Fig. S9 H/C vs. O/C in SOA formed from different aromatic hydrocarbon photooxidation under low NO_x colored by aromatic isomer type and marked with individual aromatic hydrocarbon species (C8 and C9 on the lower left indicate the location of initial aromatic hydrocarbon precursor; dashed/solid line indicate that changes between precursor and SOA components): Ethylbenzene 2084A; Propylbenzene 1245A; Isopropylbenzene 1247A; *m*-Xylene 1191A; *m*-Ethyltoluene 1199A; *o*-Xylene 1320A; *o*-Ethyltoluene 1179A; *p*-Xylene 1308A; *p*-Ethyltoluene 1194A; 1, 2, 3-Trimethylbenzene (123TMB) 1162A;1, 2, 4-Trimethylbenzene(124TMB) 1119A; 1, 3, 5-Trimethylbenzene(135TMB) 1156A. Alkyl number trend is the liner fitting in (Li., et al., 2015a).

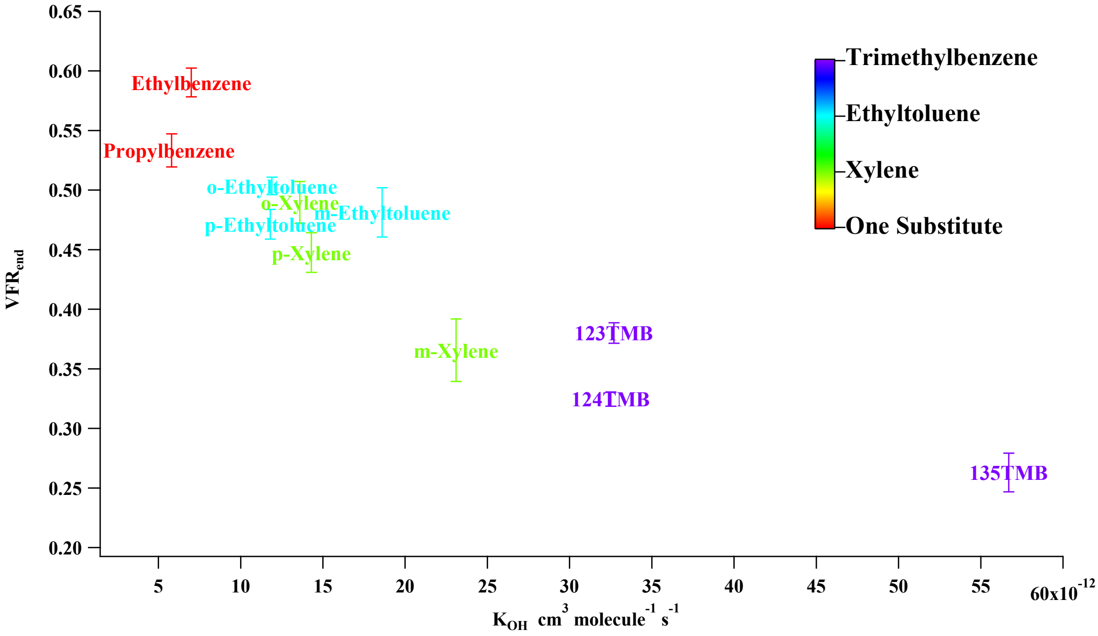

Fig S10 Relationship between VFR and K_{OH} during aromatic hydrocarbon photooxidation under low NO_x